IEEE Access
Multidisciplinary | Rapid Review | Open Access Journal

Received January 19, 2021, accepted February 3, 2021, date of publication February 9, 2021, date of current version February 18, 2021.

Digital Object Identifier 10.1109/ACCESS.2021.3058194

A Novel Capacitive Cross-Coupling Structure for Ceramic-Filled Cavity Filters

ZHENGJUN DU, JIN PAN, MA BOYUAN, XINYANG JI, AND DEQIANG YANG, (Member, IEEE)

School of Electronic Science and Engineering, University of Electronic Science and Technology of China, Chengdu 611731, China

Corresponding author: Jin Pan (jpuestc@163.com)

This work was supported in part by the Foundation for Innovative Research Group of the National Natural Science Foundation of China under Grant 6172101.

ABSTRACT Since the probe coupling for cavity filters is unsuitable for ceramic-filled cavity filters, a novel capacitive cross-coupling structure is proposed to improve stopband suppression by introducing transmission zeros. This structure is implemented by first etching a coupling window on the silver-plated layer on the ceramic surface between two resonant cavities and then placing an isolated metal strip in the window. This structure enjoys high design freedom. Thus, the coupling coefficient between the two cavities is readily adjusted. Moreover, the structure has the advantages of a compact size and simple fabrication and tuning processes. For validation, a ten-pole ceramic-filled cavity filter for 5G applications is designed and evaluated. The proposed cross-coupling technology is used to introduce a pair of symmetrical transmission zeros at the band skirts to increase the frequency selectivity. The measured results are consistent with the simulated ones.

INDEX TERMS Capacitive cross-coupling, ceramic-filled filter, stopband rejection, transmissions zeros (TZs).

I. INTRODUCTION

Stopband suppression has always been a major concern for filter design. In the past few decades, the cross-coupling technology has been popular due to its ability to obtain prescribed transmission zeros (TZs) close to the band edge for higher selectivity without increasing the number of resonant units [1]–[6]. It also has the advantages of low insertion loss, small size, low cost, etc. [7]–[11]. In [11], the multipath coupling technique was used to explain the principle of the TZs generated in the cascade triptych (CT) and cascade quadruple (CQ) topologies. According to the principle, either capacitive or inductive coupling can be introduced between nonadjacent cavities as the cross-coupling to achieve the TZs, when the main coupling channel is coupled through the magnetic field. The capacitive cross-coupling can produce a pair of symmetrical TZs in the upper and lower skirts in a CQ filter. For the CT case, either inductive or capacitive coupling can produce one TZ beyond the passband.

There have been a lot of cross-coupling techniques published for different types of filters. For inline cavity filters, the method in [12] to obtain the capacitive coupling was by simply rotating the third resonator. In [13], an approach of distributed cross-coupling was designed with an aperture connecting the orthogonal coaxial cavity filters. Its capacitive coupling was realized by the discs coupled to the port. There were some difficulties existing in the techniques, including hardly controllable coupling coefficients, and deficient TZs in both sides of the passband.

For folded cavity filters, the cross-coupling was usually implemented by capacitive-coupling probes [14]–[19]. The common difficulties encountered in probe-coupling techniques are in-band response degrading, unguaranteed coupling precision, and so on. For waveguide cavity filters, although this kind of structure was simple, the coupling coefficient is not precisely controllable, the accuracy of manufacturing was not guaranteed, and much tuning work was required in post-processing [18]. For filters based on printed circuits [19], the coupling patch and strip were used to generate the TZs. The precision is significantly improved.

With the commercialization of 5G communication technology, ceramic-filled cavity filters have become the mainstream solution for the usage of filters in 5G applications. The ceramic-filled cavity filters have the advantages of small size, lightweight, low cost, and low-temperature drift. So far, studies on the implementation of capacitive cross-coupling

The associate editor coordinating the review of this manuscript and approving it for publication was Guido Valerio.

for ceramic-filled cavity filters are insufficient. Little work on this subject can be founded in publications. The relevant researches most close to the subject were about cross-coupling methods used in dielectric-loaded resonator filters, or about designs of the dielectric filter without usages of cross-coupling [20]–[30]. For the dielectric-loaded resonator filter, the aforementioned cross-coupling techniques could principally be used to achieve the needed TZs because its resonator cavity space been only occupied partly by dielectrics. But for the case of ceramic-filled cavity filters, each resonator cavity space is fully occupied by dielectrics, no space left for other structures intervened to implement cross-coupling.

In this paper, a capacitive cross-coupling structure is proposed for ceramic-filled cavity filters. The proposed structure is implemented on the silver-coated surface of the ceramic filter. It owns a simple fabrication process, and excellent tuning flexibility and accuracy. It is applicable to mass production and capable of achieving adjustable TZs as well. With the proposed structure, a ten-pole ceramic-filled filter suitable for 5G applications is designed and fabricated for performance examination.

In Section II, the capacitive coupling principle of the proposed structure is explained by analyzing the field distribution in and between each resonant cavity. Moreover, the method to identify the coupling characteristic of the structure is given by the equivalent circuits for cross-coupling. The technique of generating TZs based on the proposed is discussed in Section III. The fabrication and measurement of the filter prototype are presented in Section IV. Finally, the conclusions are given in Section V.

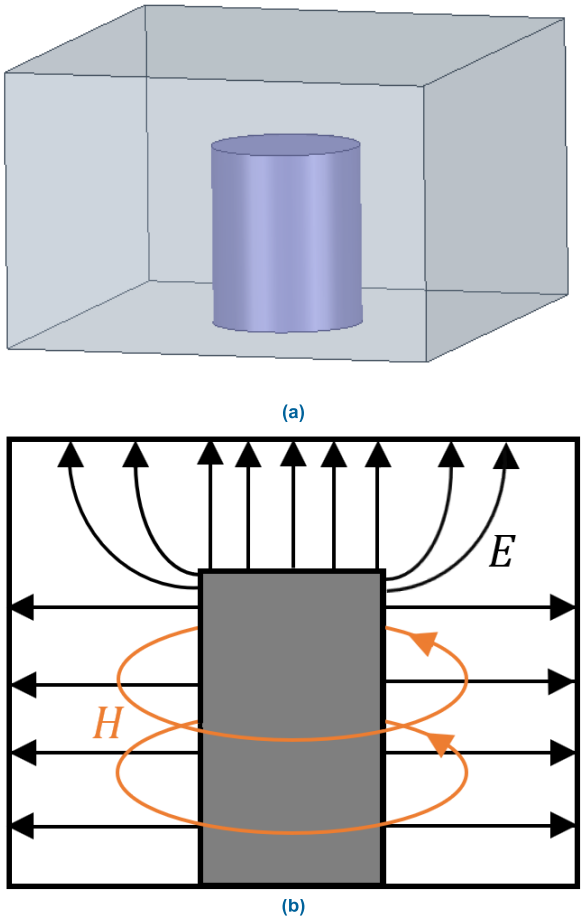

FIGURE 1. (a) Implementation of the resonant cavity. (b) The field distribution of the resonant cavity.

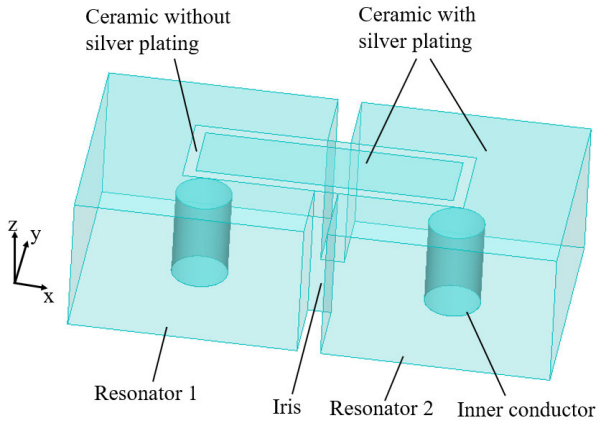

FIGURE 2. Implementation of the proposed cross-coupling structure.

II. CAPACITIVE CROSS-COUPLING PRINCIPLE OF THE PROPOSED STRUCTURE

A. THE COUPLING STRUCTURE AND ITS PRINCIPLE

A capacity-loaded miniaturized quasi-$\lambda/4$ coaxial cavity resonator is shown in Fig. 1 (a). The cavity consists of a ceramic body with silver-coated surfaces. The inner conductor is implemented by the silver-coated circular blind holes embedded in the ceramic bulk. This configuration has excellent compatibility with general fabrication and processing technologies for ceramic blocks. The EM field distributions of the resonator fundamental mode are shown in Fig. 1 (b). The bottom end of the center inner conductor is shorted. The gap between the top end of the inner conductor and the metallic silver surface introduces capacitive loading to the resonator [31]-[33]. As a result, the electric field concentrates within the gap intensely. A circumferential magnetic field encircles the inner conductor and aggregates at the shorted end [34].

As we know, the probe-based capacitive-coupling buried inside cavities is unsuitable for solid ceramic filters. Therefore, a novel capacitive coupling structure is hereby proposed, as shown in Fig. 2. The capacitive coupling is implemented on the surface of the silver-plated ceramic. An isolated metal strip for coupling is placed within a window etched on the silver surface. It is located on the top outside surface of the capacity-loaded end of the resonators, where the concentrated gap electric fields are mainly normal to the coupling strip. Therefore, the strip plays a role of the capacitive-coupling substructure connecting the two cavities to be coupled. Besides, for the convenience of the structure stability and fabrication feasibility, the originally apart two nonadjacent resonators to be coupled are cut-through with ceramic to hold the etched coupling window. Therefore, accompanied by

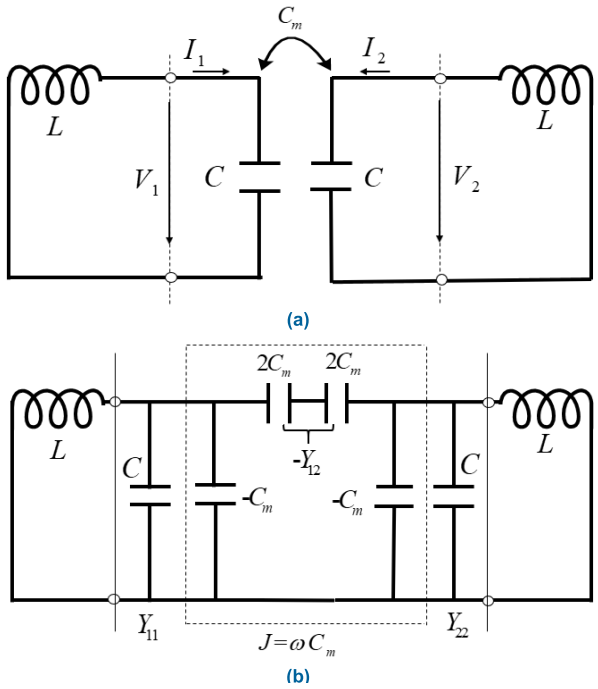

FIGURE 3. (a) Coupled resonance circuit with electric coupling. (b) An alternative form of the equivalent circuit using an admittance inverter $J = \omega C_m$ to represent the coupling structure.

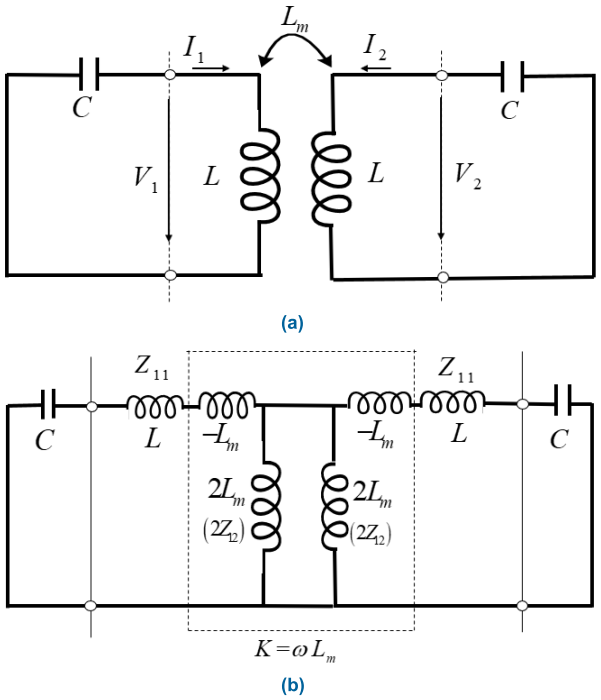

FIGURE 4. (a) Coupled resonance circuit with magnetic coupling. (b) An alternative form of the equivalent circuit using an impedance inverter $K = \omega L_m$ to represent the coupling structure.

the cutting through, an additional inductive coupling channel is introduced by the inter-cavity opening (iris) under the strip. It is obvious that the width of the iris should be small to ensure the capacitive coupling predominates. With the proposed composite structure, the coupling strength is readily adjusted by varying the dimension of the strip, which supports the flexible design of TZs.

B. IDENTIFICATION OF COUPLING CHARACTERISTICS OF THE PROPOSED STRUCTURE

The presented cross-coupling structure is a combination of both capacitive and inductive parts. The metal strip mainly introduces electric coupling, whereas the openings in the cavity wall (iris) leads to magnetic coupling [35]. Therefore, the dimensions of the structure may influence its coupling characteristics and performance. Hereon the equivalent circuit for two coupled resonators is used to identify the coupling characteristic of the structure with different dimensions. For the case of two capacitive-coupling resonant cavities, its equivalent circuit is shown in Figs. 3 (a) and 3 (b) [36]. The capacitive coupling can be represented by an admittance inverter, $J = \omega C_m$. Since the circuit is in a symmetric form, the odd-even mode can be used to analyze the coupling characteristics. The frequencies of the odd and even modes, respectively, are

$$f_{od} = 1\Big/\left(2\pi\sqrt{L(C+C_m)}\right) \tag{1}$$

$$f_{ev} = 1\Big/\left(2\pi\sqrt{L(C-C_m)}\right) \tag{2}$$

The capacitive coupling coefficient is defined as

$$k_E = \left(f_{ev}^2 - f_{od}^2\right)\Big/\left(f_{od}^2 + f_{ev}^2\right) \tag{3}$$

For a pair of coupled microwave resonators, the above coupling coefficient could be obtained through the eigenmode solver in Ansys High Frequency Structure Simulator (HFSS).

It can be seen from the formulas (1) and (2) that the resonant frequency of the odd mode is lower than that of the even mode for the capacitive-coupling case.

For the case of two inductively-coupled resonators, its equivalent circuit is similar and as shown in Figs. 4 (a) and 4 (b) [36]. Its inductive coupling can be represented by an impedance inverter, $K = \omega L_m$. The resonant frequencies of the odd and even modes, respectively, are

$$f_{od} = 1\Big/\left(2\pi\sqrt{(L-L_m)C}\right) \tag{4}$$

$$f_{ev} = 1\Big/\left(2\pi\sqrt{(L+L_m)C}\right) \tag{5}$$

The inductive coupling coefficient is defined as

$$k_M = \left(f_{od}^2 - f_{ev}^2\right)\Big/\left(f_{od}^2 + f_{ev}^2\right) \tag{6}$$

It can be seen from formulas (4) and (5) that the resonant frequency of the even mode is lower than that of the odd mode for this case.

The above analysis tells us that the resonance frequencies of odd and even modes can be used to characterize the coupling structure.

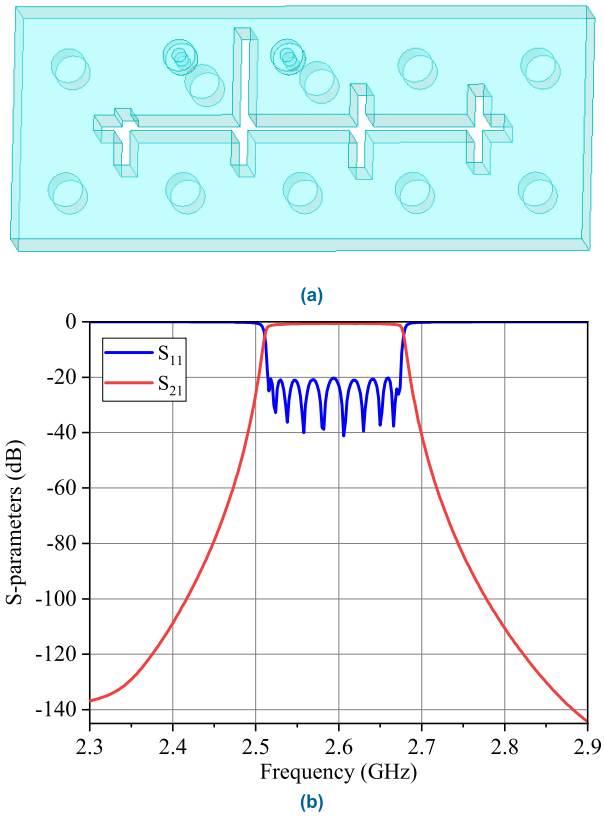

FIGURE 5. (a) The ten-pole filter without a cross-coupling structure. (b) The S-parameters of the ten-pole filter without a cross-coupling structure.

III. DESIGN OF TZs WITH THE PROPOSED CROSS-COUPLING STRUCTURE

A. DESIGN OF A CERAMIC-FILLED CAVITY FILTER

A ten-pole ceramic-filled cavity filter is designed for 5G applications. The simulation model and filtering performance of the filter without a cross-coupling structure are shown in Figs. 5 (a) and 5 (b), respectively. The in-band insertion loss (IL) and return loss (RL) are −2.2 dB and −20 dB, respectively. Stopband suppression cannot meet the requirement of the 5G communication system. To enhance the stopband suppression, we can set the proposed capacitive coupling structure between the sixth and ninth cavities to introduce TZs. The simulation model and topology of the filter are presented in Figs. 6 (a) and 6 (b), respectively. The dashed line in Fig. 6 (b) shows the capacitive coupling route and solid lines show the inductive coupling ones.

B. PARAMETRIC ANALYSIS

The proposed cross-coupling structure contains both capacitive and inductive coupling channels. The coupling characteristics could be easily overturned through dimensional changes. In the following, we will first study the influence of the strip dimension changes on the coupling characteristics with a constant width of the iris. After that, the affections of iris width changes will be considered with the constant strip dimensions.

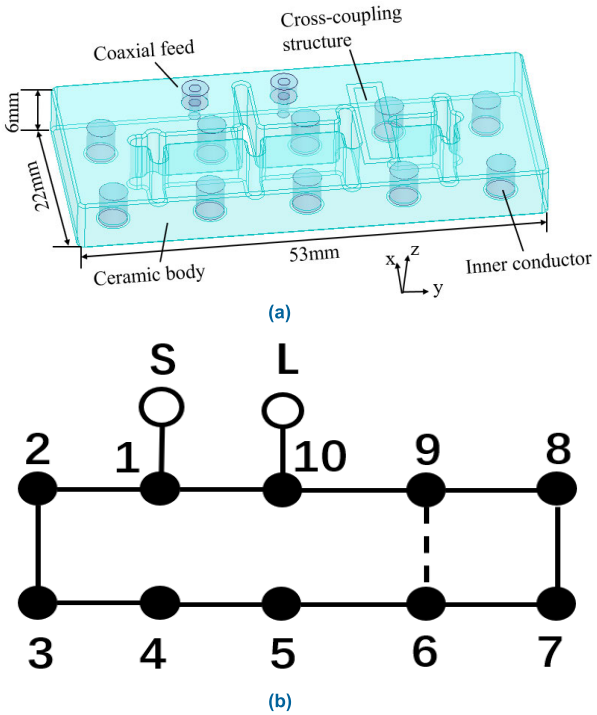

FIGURE 6. (a) The ten-pole filter with a cross-coupling structure. (b) The topological structure of the ten-pole filter.

TABLE 1. The research scheme of the coupling structure size (The electrical length at 2.6 GHz).

	Scheme 1	Scheme 2	Scheme 3	Scheme 4
a (λ)	1.7×10^{-3} - 1.7×10^{-2}	8.7×10^{-3}	8.7×10^{-3}	8.7×10^{-3}
b (λ)	8.7×10^{-3}	1.7×10^{-3} - 1.7×10^{-2}	8.7×10^{-3}	8.7×10^{-3}
c (λ)	2.6×10^{-2}	2.6×10^{-2}	1.7×10^{-2} - 3.4×10^{-2}	2.6×10^{-2}
d (λ)	8.7×10^{-2}	8.7×10^{-2}	8.7×10^{-2}	5.2×10^{-2} - 0.13

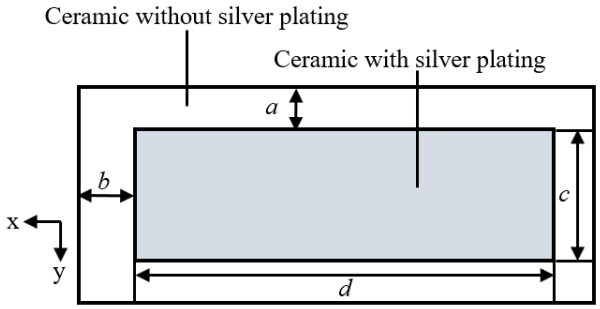

FIGURE 7. The size parameters of the cross-coupling structure.

It is shown in Table 1 that we set four rounds of parameter scanning schemes to analyze strip dimension affections. In each scheme, we scan only one parameter within a certain range while keeping others constants. As shown in Fig. 7, a and b are the slot widths between the metal strip and window edges, respectively; c and d are the width and length of the metal strip, respectively.

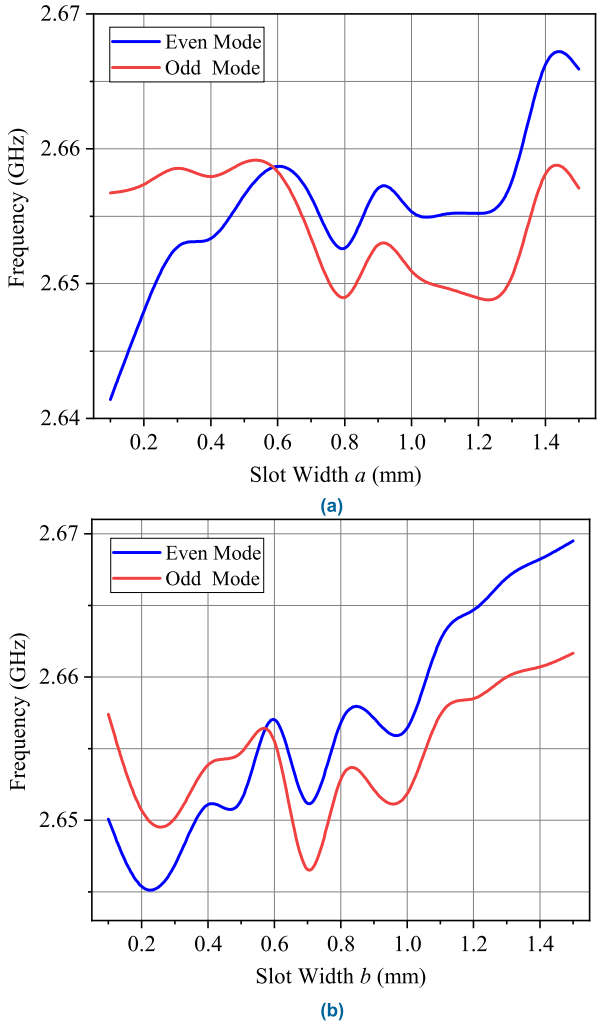

FIGURE 8. (a) The influence of the slot width *a* on the frequency of the odd and even modes. (b) The influence of the slot width *b* on the frequency of the odd and even modes.

The influence of the slot widths a and b on the odd and even modes is shown in Figs. 8 (a) and 8 (b). The resonant frequency of the odd mode approaches that of the even mode as the width of the slot increases. When the odd mode has a lower resonant frequency than the even mode, coupling turns from inductive to capacitive. When the slot widths a and b are in the range of 0.005λ to 0.014λ, capacitive coupling dominates. Hence, the slot widths a and b can be set as the same value to simplify the design.

The influence of the metal width c and length d on the odd and even modes is shown in Figs. 9 (a) and 9 (b). When the even mode has a higher resonant frequency than the odd mode, the coupling is capacitive. In this case, the width of the metal strip is in the range of 0.023λ to 0.026λ, and the length of the metal strip is in the range of 0.084λ to 0.122λ. Thus, the length of the metal strip is flexible. It can be used for tuning.

The influence of the iris width on the odd and even modes is shown in Fig. 10. When the width of the iris is at the range of 0.035λ to 0.055λ, the capacitive coupling is still ensured.

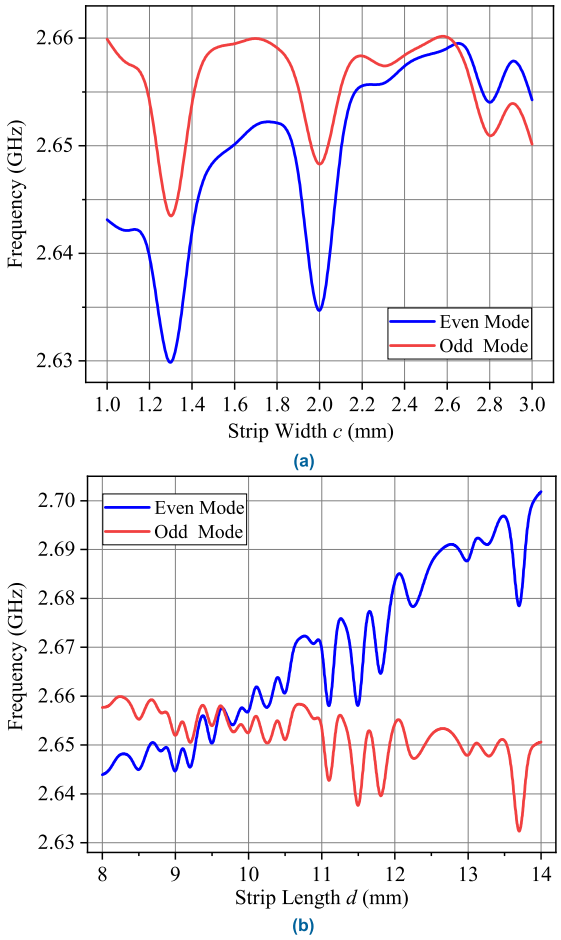

FIGURE 9. (a) The influence of the metal strip width on the frequency of the even and odd modes. (b) The influence of the metal strip length on the frequency of the even and odd modes.

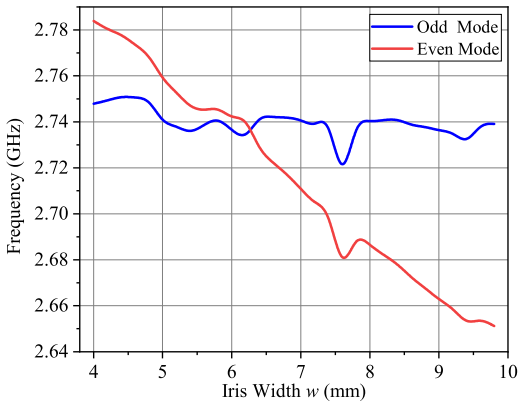

FIGURE 10. The influence of the iris width on the frequency of the even and odd modes.

The transition between inductive and capacitive coupling is presented in Table 2.

C. INFLUENCE OF THE STRUCTURE POSITION ON THE COUPLING CHARACTERISTICS

When the cross-coupling structure is offset along the y-axis as shown in Fig. 11 (a), the influence of the strip length on the odd and even modes is shown in Fig. 11 (b), which shows that

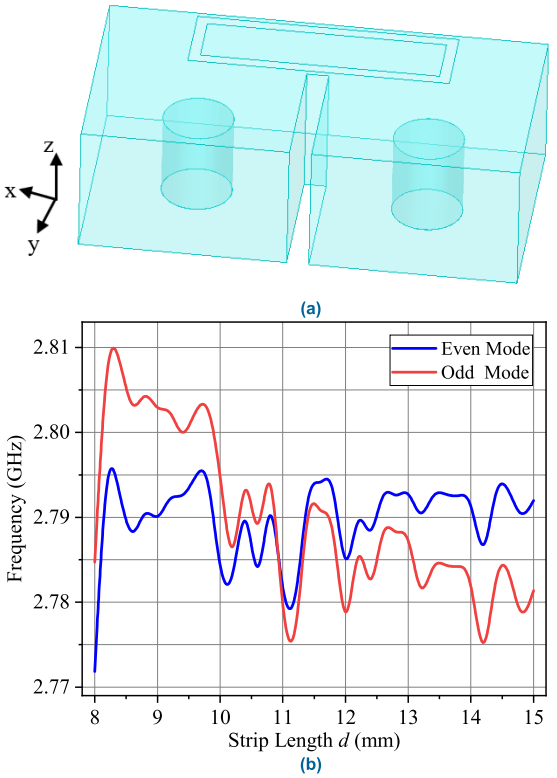

FIGURE 11. (a) Offset cross-coupling structure along the y-axis. (b) The influence of the strip length on the odd and even modes.

TABLE 2. Transition between inductive or capacitive coupling (The electrical length at 2.6 GHz).

	Inductive	Capacitive
a	0.002 λ - 0.004 λ	0.005 λ - 0.014 λ
b	0.002 λ - 0.004 λ	0.005 λ - 0.014 λ
c	0.009 λ - 0.023 λ	0.024 λ - 0.026 λ
d	0.07 λ - 0.083 λ	0.084 λ - 0.122 λ
w	0.056 λ - 0.085 λ	0.035 λ - 0.055 λ

the coupling is capacitive if the length of the metal strip is in the range of 0.096λ to 0.13λ. The simulation results tell us that only a longer metal strip may ensure capacitive coupling if the structure moves along the y-axis. This conclusion coincides with the physical property of the sparse electric field distributions at the location of the coupling structure.

When the cross-coupling structure moves along the x-axis, as seen in Fig. 12 (a), the simulation results in Fig. 12 (b) show that the capacitive coupling can be still ensured if the offset distance is less than 0.013λ. As the structure position changes, the transition between the inductive and capacitive coupling is shown in Table 3.

D. OPTIMAL DESIGN OF THE STOPBAND TZs

The filter with the capacitive cross-coupling structure in Fig. 6 (a) is designed and optimized. The optimized design is implemented in HFSS and CST. The tuning method of the resonance frequency and coupling coefficients are shown in

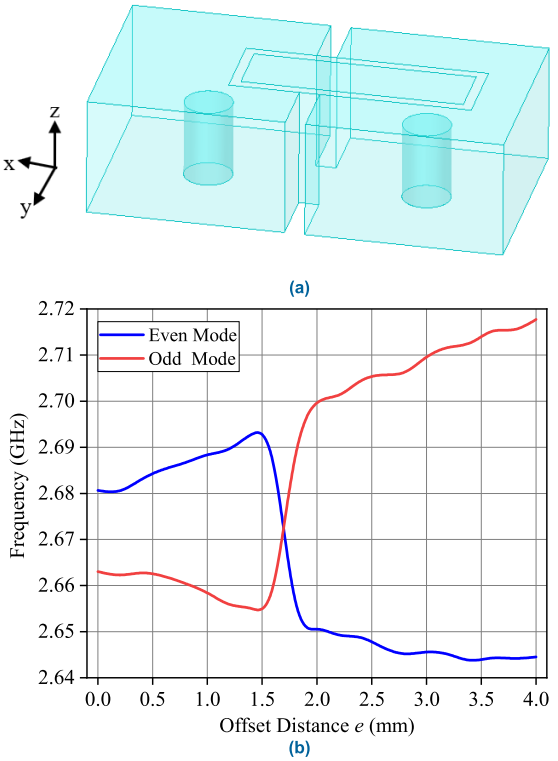

FIGURE 12. (a) Offset cross-coupling structure along the x-axis. (b) The influence of the cross-coupling structure moves along the x-axis on odd and even modes.

TABLE 3. The influence of the position on coupling characteristic (The electrical length at 2.6 GHz).

	Inductive	Capacitive
Off along y-axis	0.069 λ - 0.095 λ	0.096 λ - 0.13 λ
Off along x-axis	> 0.014 λ	< 0.013 λ

TABLE 4. The frequency responses of the different strip lengths.

Coupling Strip Length d (mm)	12.3	12.88	13.3
TZs (GHz)	2.49/2.7	2.5/2.69	2.5/2.68
Return Loss (dB)	-20	-20	-20
Insertion Loss (dB)	-2.38	-2.14	-2.78

Figs. 13 (a), 13 (b) and 13 (c). The optimized parameters are $a = b = 0.013\lambda$, $c = 0.035\lambda$, and $d = 0.12\lambda$. The length and width of the filter are 0.46λ and 0.19λ, respectively. The height is 0.05λ. The frequency responses are shown in Fig. 14. A pair of symmetrical TZs are introduced at the band skirts to increase the frequency selectivity. The first and tenth cavities are connected to improve structural robustness.

The frequency selectivity can be optimized by adjusting the length of the metal strip, as shown in Fig. 15. The longer length of the metal strip is, the stronger suppression of the stopband becomes. However, this could affect the in-band response. The frequency responses obtained with different strip lengths are shown in Table 4. Both the in-band response and stopband selectively should be considered.

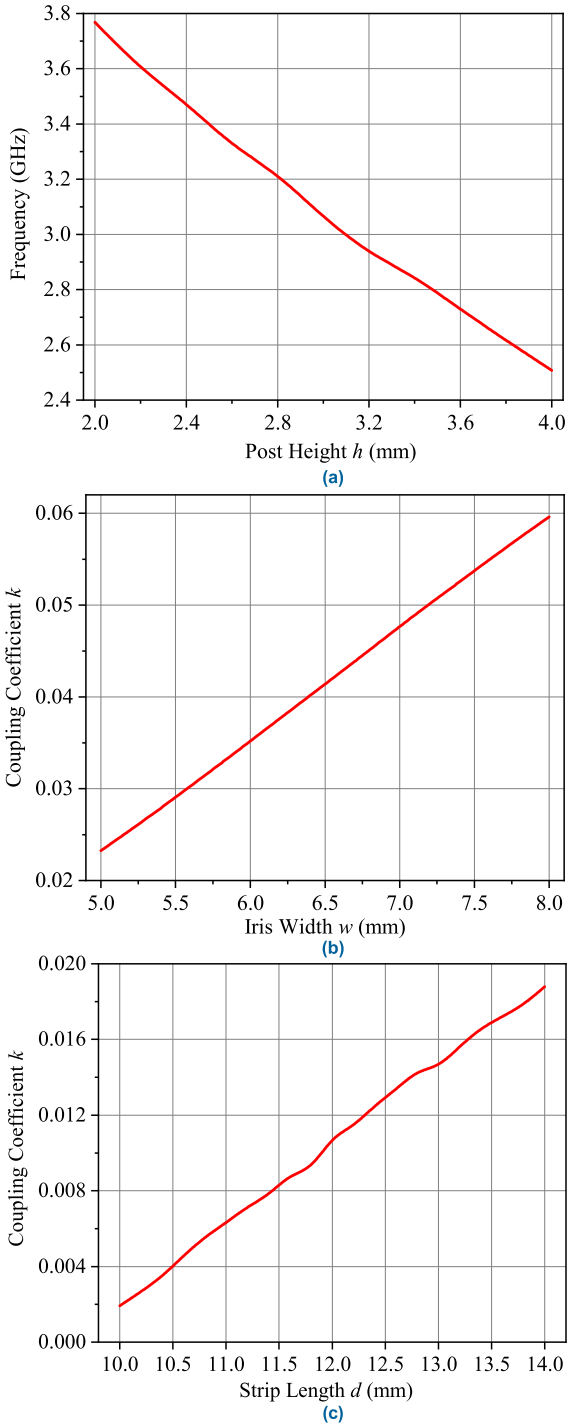

FIGURE 13. (a) The influence of the post height on frequency. (b) The influence of the iris width on coupling coefficient. (c) The influence of the strip length on cross-coupling coefficient.

IV. FILTER FABRICATION AND MEASURED RESULTS

For validation, the ten-pole ceramic-filled cavity filter was fabricated, as shown in Fig. 16 (a). The fabrication accuracy of the ceramic block and silver plating are 0.01 mm and 0.02 mm, respectively. The permittivity and loss tangent of the ceramic are 20.5 and 1.4×10^{-4}, respectively. The hardware tuning is based on the vector network analyzer (VNA)

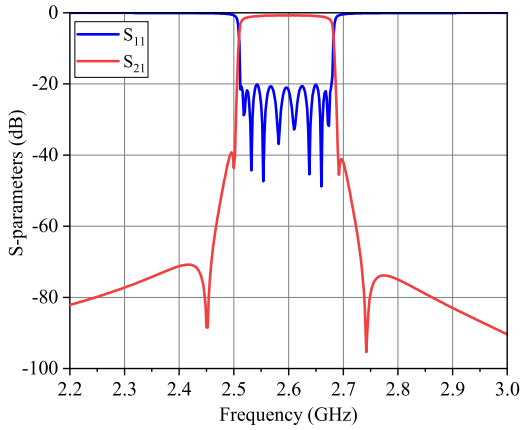

FIGURE 14. S-parameters of the ten-order ceramic-filled cavity filter with a capacitive cross-coupling structure.

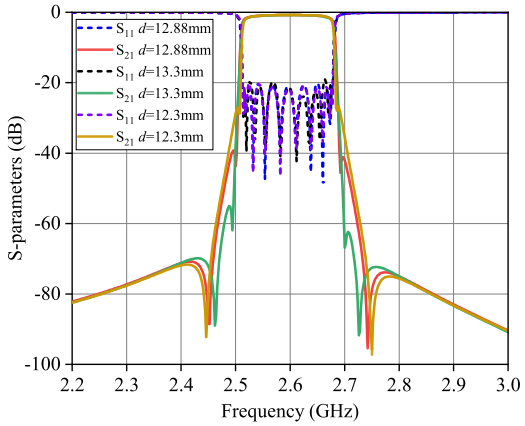

FIGURE 15. Frequency responses of ten-pole ceramic-filled cavity filter with different lengths of coupling strips.

and the software CST. The S-parameters are obtained by the VNA. The CST presents the tuning guide after loading the S-parameters. The tuning law presented in Figs. 13 (a), 13 (b) and 13 (c) is applied.

The tuning for individual cavities is implemented by drilling the notches of each cavity, i.e., the inner conductor. The tuning of the inductive coupling is done by adjusting the width of the iris through machining. The solid structure makes the tuning process irreversible. However, the proposed capacitive cross-coupling structure enjoys superior tuning flexibility. The dimension of the silver-plated strip is adjusted through etching and printing.

The center frequency and bandwidth of the filter are 2.6 GHz and 160 MHz, respectively. The worst in-band RL and IL of the filter are −19 dB and −2.2 dB, respectively. The frequencies of two symmetric TZs are 2.5 and 2.69 GHz, respectively. The measured and simulated S-parameters of the ten-order filter are presented in Fig. 16 (b). The results are consistent, thus verifying the design. A comparison between the capacitive cross-coupling for cavity filters with the state-of-the-arts is shown in Table 5. It reveals that this filter has the merits of higher selectively, wide bandwidth and compact size.

TABLE 5. The comparison of state-of-the-art cavity filters with cross-coupling.

Ref	[13]	[17]	[18]	[26]	**This work**
Technology	Orthogonal Coaxial Cavity	Coaxial Cavity	Waveguide Cavity	Dielectric-loaded Cavity	**Ceramic-filled Cavity**
Cross-coupling	Aperture	Rotated Rod	Inline Probe	U-shape Probe	**Metal Strip**
Order	3	4	4	4	**10**
f_0 (GHz)	2.14	2.02	10	2.595	**2.595**
FBW (%)	0.7	0.7	0.4	1.9	**6.2**
IL (dB)	N/A	0.72	0.8	0.4	**2.2**
RL (dB)	25	23	20	20	**20**
Stopband Rejection	>35 dB up to 1.1 f_0	>30 dB up to 6.3 f_0	>30 dB up to 1.47 f_0	>30 dB up to 1.4 f_0	**> 40 dB up to 2 f_0**
Unloaded Q	2700	3400	7300	3000	**1400**
Size (λ)	0.19*0.19*0.57	0.67*0.57*0.2	1.27*1.27*3.13	0.47*0.47*0.15	**0.46*0.17*0.05**

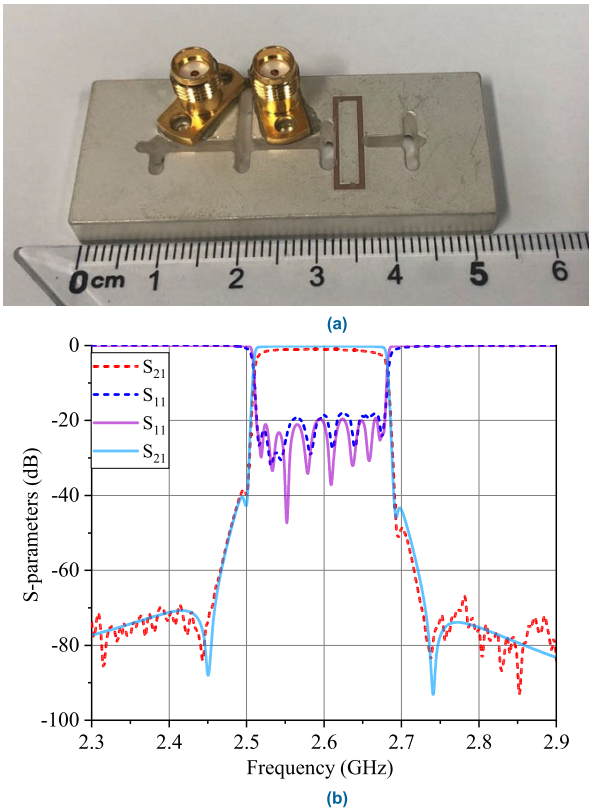

FIGURE 16. (a) The fabricated ten-pole ceramic-filled cavity filter. (b) The measured S-parameters of the ten-pole ceramic-filled cavity filter. Dashed lines: measured results. Solid lines: simulation results.

V. CONCLUSION

A novel capacitive cross-coupling structure implemented in ceramic-filled cavity filters has been proposed to increase frequency selectivity. The characteristic of the proposed coupling structure has been studied based on the odd-even mode analysis. The transition between capacitive and inductive coupling has been discussed. It has been proven that the proposed structure possesses excellent tuning flexibility. This facilitates the design of TZs and ensures their precision. A ten-pole ceramic-filled cavity filter has been designed and fabricated for 5G applications. The measured results agree well with the simulation results.

REFERENCES

[1] R. J. Cameron, "General coupling matrix synthesis methods for Chebyshev filtering functions," *IEEE Trans. Microw. Theory Techn.*, vol. 47, no. 4, pp. 433–442, Apr. 1999.
[2] R. Levy, "Filters with single transmission zeros at real or imaginary frequencies," *IEEE Trans. Microw. Theory Techn.*, vol. MTT-24, no. 4, pp. 172–181, Apr. 1976.
[3] A. E. Atia and A. E. Williams, "Narrow-bandpass waveguide filters," *IEEE Trans. Microw. Theory Techn.*, vol. MTT-20, no. 4, pp. 258–265, Apr. 1972.
[4] S. Amari and M. Bekheit, "New dual-mode dielectric resonator filters," *IEEE Microw. Wireless Compon. Lett.*, vol. 15, no. 3, pp. 162–164, Mar. 2005.
[5] I. Awai, A. C. Kundu, and T. Yamashita, "Equivalent-circuit representation and explanation of attenuation poles of a dual-mode dielectric-resonator bandpass filter," *IEEE Trans. Microw. Theory Techn.*, vol. 46, no. 12, pp. 2159–2163, Dec. 1998.
[6] F. Cheng, X. Q. Lin, M. Lancaster, K. Song, and Y. Fan, "A dual-mode substrate integrated waveguide filter with controllable transmission zeros," *IEEE Microw. Wireless Compon. Lett.*, vol. 25, no. 9, pp. 576–578, Sep. 2015.
[7] M. A. Sanchez-Soriano, S. Sirci, J. D. Martinez, and V. E. Boria, "Compact dual-mode substrate integrated waveguide coaxial cavity for bandpass filter design," *IEEE Microw. Wireless Compon. Lett.*, vol. 26, no. 6, pp. 386–388, Jun. 2016.
[8] S.-W. Wong, R.-S. Chen, J.-Y. Lin, L. Zhu, and Q.-X. Chu, "Substrate integrated waveguide quasi-elliptic filter using slot-coupled and microstrip-line cross-coupled structures," *IEEE Trans. Compon., Packag., Manuf. Technol.*, vol. 6, no. 12, pp. 1881–1888, Dec. 2016.
[9] X.-P. Chen and K. Wu, "Substrate integrated waveguide cross-coupled filter with negative coupling structure," *IEEE Trans. Microw. Theory Techn.*, vol. 56, no. 1, pp. 142–149, Jan. 2008.
[10] D. L. Diedhiou, E. Rius, J.-F. Favennec, and A. El Mostrah, "Ku-band cross-coupled ceramic SIW filter using a novel electric cross-coupling," *IEEE Microw. Wireless Compon. Lett.*, vol. 25, no. 2, pp. 109–111, Feb. 2015.
[11] J. B. Thomas, "Cross-coupling in coaxial cavity filters—A tutorial overview," *IEEE Trans. Microw. Theory Techn.*, vol. 51, no. 4, pp. 1368–1376, Apr. 2003.
[12] Y. Wang and M. Yu, "True inline cross-coupled coaxial cavity filters," *IEEE Trans. Microw. Theory Techn.*, vol. 57, no. 12, pp. 2958–2965, Dec. 2009.
[13] M. Hoft and F. Yousif, "Orthogonal coaxial cavity filters with distributed cross-coupling," *IEEE Microw. Wireless Compon. Lett.*, vol. 21, no. 10, pp. 519–521, Oct. 2011.

[14] C. Wang and K. A. Zaki, "Full wave modeling of electric coupling probes in combline resonators and filters," in *IEEE MTT-S Int. Microw. Symp. Dig.*, Boston, MA, USA, Jun. 2000, pp. 1649–1652.

[15] C. Wang and K. A. Zaki, "Full-wave modeling of electric coupling probes in comb-line resonators and filters," *IEEE Trans. Microw. Theory Techn.*, vol. 48, no. 12, pp. 2459–2464, Dec. 2000.

[16] Y. Chen and K.-L. Wu, "An all-metal capacitive coupling structure for coaxial cavity filters," in *IEEE MTT-S Int. Microw. Symp. Dig.*, Los Angeles, CA, USA, Aug. 2020, pp. 583–586, doi: 10.1109/IMS30576.2020.9223932.

[17] M. Hoft, "Tunable capacitive coupling for cavity resonator filters," in *Proc. German Microw. Conf.*, Munich, Germany, Mar. 2009, pp. 1–4.

[18] M. Latif, G. Macchiarella, and F. Mukhtar, "A novel coupling structure for inline realization of cross-coupled rectangular waveguide filters," *IEEE Access*, vol. 8, pp. 107527–107538, 2020.

[19] B. Mohajer-Iravani and M. A. EL Sabbagh, "High-selective wide-band combline filters based on miniaturized-engineered resonators, inter-resonator tapped-in coupling, and probe coupling," in *Proc. IEEE Radio Wireless Symp.*, Santa Clara, CA, USA, Jan. 2012, pp. 307–310.

[20] C. Wang, K. A. Zaki, A. E. Atia, and T. Dolan, "Dielectric combline resonators and filters," in *IEEE MTT-S Int. Microw. Symp. Dig.*, Baltimore, MD, USA, Jun. 1998, pp. 1315–1318.

[21] C. Wang, K. A. Zaki, A. E. Atia, and T. G. Dolan, "Dielectric combline resonators and filters," *IEEE Trans. Microw. Theory Techn.*, vol. 46, no. 12, pp. 2501–2506, Dec. 1998.

[22] X.-F. Liang and W. D. Blair, "High Q TE01 mode DR cavity filters for wireless base stations," in *IEEE MTT-S Int. Microw. Symp. Dig.*, Baltimore, MD, USA, Jun. 1998, pp. 825–828.

[23] J.-F. Liang and W. D. Blair, "High-Q TE01 mode DR filters for PCS wireless base stations," *IEEE Trans. Microw. Theory Techn.*, vol. 46, no. 12, pp. 2493–2500, Dec. 1998.

[24] X.-G. Sun, W.-Z. Li, and L. Ge, "Dielectric loaded cavity filter with wide spurious free region and better out-of-band rejection," in *Proc. Asia–Pacific Microw. Conf.*, Yokohama, Japan, Dec. 2006, pp. 1200–1203.

[25] V. Walker and I. C. Hunter, "Design of cross-coupled dielectric-loaded waveguide filters," *IEE Proc.-Microw., Antennas Propag.*, vol. 148, no. 2, pp. 91–96, Apr. 2001.

[26] X. Wang and K. Wu, "A TM01 mode monoblock dielectric filter," *IEEE Trans. Microw. Theory Techn.*, vol. 62, no. 2, pp. 275–281, Feb. 2014.

[27] J. Jiang and R. R. Mansour, "Wideband dielectric substrate-loaded cavity filter," *IEEE Trans. Microw. Theory Techn.*, vol. 68, no. 1, pp. 111–120, Jan. 2020.

[28] R. Zhang and R. R. Mansour, "Dual-band dielectric-resonator filters," *IEEE Trans. Microw. Theory Techn.*, vol. 57, no. 7, pp. 1760–1766, Jul. 2009.

[29] S. Afridi, U. Ahmed, A. R. Gilal, J. Jaafar, I. A. Aziz, and M. Y. Sandhu, "High stop band rejection for ceramic loaded waveguide filters," *IEEE Access*, vol. 8, pp. 109309–109314, 2020.

[30] R. Zhang and R. R. Mansour, "Low-cost dielectric-resonator filters with improved spurious performance," *IEEE Trans. Microw. Theory Techn.*, vol. 55, no. 10, pp. 2168–2175, Oct. 2007.

[31] R. J. Cameron, R. Mansour, and C. M. Kudsia, *Microwave Filters for Communication Systems: Fundamentals, Design and Applications*. Hoboken, NJ, USA: Wiley, 2007.

[32] J.-S. G. Hong and M. J. Lancaster, *Microstrip Filters for RF/Microwave Applications*. New York, NY, USA: Wiley, 2011.

[33] I. C. Hunter, *Theory and Design of Microwave Filters*. London, U.K.: IEE, 2001.

[34] J.-S. Zhan and J.-L. Wang, "A simple four-order cross-coupled filter with three transmission zeros," *Prog. Electromagn. Res. C*, vol. 8, pp. 57–68, 2009, doi: 10.2528/PIERC09041107.

[35] A. Anand and X. Liu, "Reconfigurable planar capacitive coupling in substrate-integrated coaxial-cavity filters," *IEEE Trans. Microw. Theory Techn.*, vol. 64, no. 8, pp. 2548–2560, Aug. 2016.

[36] J.-S. Hong and M. J. Lancaster, "Couplings of microstrip square open-loop resonators for cross-coupled planar microwave filters," *IEEE Trans. Microw. Theory Techn.*, vol. 44, no. 11, pp. 2099–2109, Nov. 1996.

ZHENGJUN DU was born in Linyi, Shandong, China, in 1990. He received the B.S. degree in electronic information engineering from the School of Science, Linyi University of China, Linyi, in 2015. He is currently pursuing the master's degree with the University of Electronic Science and Technology of China, Chengdu, China. His current research interest includes theory and the design of dielectric filter.

JIN PAN received the B.S. degree in electronics and communication engineering from the Radio Engineering Department, Sichuan University, Chengdu, China, in 1983, and the M.S. and Ph.D. degrees in electromagnetic field and microwave technique from the University of Electronic Science and Technology of China (UESTC), in 1986 and 1989, respectively. From 2000 to 2001, he was a Visiting Scholar in electronics and communication engineering from the Radio Engineering Department, City University of Hong Kong. He is currently a Full Professor with the School of Electronic Engineering, UESTC. His current research interests include electromagnetic theory and computation, antenna theory and technique, field and wave in inhomogeneous media, and microwave remote sensing theory and its applications.

MA BOYUAN was born in Changchun, Jilin, China, in 1993. He received the B.S. degree in electromagnetic field and wireless technology from the Yingcai Honors College, University of Electronic Science and Technology of China, Chengdu, China, in 2016, where he is currently pursuing the Ph.D. degree with the School of Electric Science and Engineering. His current research interest includes the theory and design of dielectric resonator antennas.

XINYANG JI was born in Luoyang, Henan, China, in 1989. He received the B.S. degree in radar engineering from the Ordnance Engineering College, Shijiazhuang, China, in 2010. He is currently pursuing the master's degree with the University of Electronic Science and Technology of China, Chengdu, China. His current research interest includes theory and the design of antenna.

DEQIANG YANG (Member, IEEE) received the B.E., M.E., and D.E. degrees from the School of Electronic Engineering, University of Electronic Science and Technology of China (UESTC), in 1992, 2006, and 2012, respectively. From 2012 to 2016, he was a Senior Engineer with UESTC. His research interests include UWB indoor localization technology, antenna measurement, and antenna theory.